We are IntechOpen,
the world's leading publisher of Open Access books
Built by scientists, for scientists

6,900
Open access books available

186,000
International authors and editors

200M
Downloads

Our authors are among the

154
Countries delivered to

TOP 1%
most cited scientists

12.2%
Contributors from top 500 universities

Interested in publishing with us?
Contact book.department@intechopen.com

Numbers displayed above are based on latest data collected.
For more information visit www.intechopen.com

The Non-Neighbor Effect in Graphene Ribbons

Tong Guo-Ping
Zhejiang Normal University
People's Republic of China

1. Introduction

Graphene is the name given to a flat monolayer of carbon atoms tightly packed into a two-dimensional honeycomb lattice (Novoselov et al., 2004), and is a rapidly rising star on the horizon of materials science and condensed matter physics. This two-dimensional material exhibits exceptionally high crystal and electronic quality and has already revealed a cornucopia of new physics and potential applications. Charge transport properties in graphene are greatly different from that of conventional two-dimensional electronic systems as a consequence of the linear energy dispersion relation near the charge neutrality point (Dirac point) in the electronic band structure (Geim & Novoselov, 2007; Novoselov et al., 2005; Zhang et al., 2005).

Theoretically, the energy band structure of a graphite monolayer had been investigated using the tight-binding approximation (Wallace, 1947). In the work of Wallace, the nearest- and next-nearest-neighbor interaction for the $2p_z$ orbitals in graphene were considered, but the wave function overlap between carbon atoms was neglected. Since his aim is to show how the π-electron distribution is related to the electrical conductivity of graphite, he did not attempt to draw the band distribution. In 1952, Coulson & Taylor considered the overlap integrals between atomic orbitals in studying the band structure of the graphite monolayer. Their work suggested that the overlap was important for the electronic density of states and referred mainly to the π states, leading to a description of the conduction band (Coulson & Taylor, 1952). To study the valence bands in graphene, Lomer used the group-threoretical method to deal with the electronic energy bands based on the three atomic orbitals $2s$, $2p_x$, and $2p_y$ (Lomer, 1955). Because there are two atoms per unit cell, there are six basis functions to be considered, and in general the tight binding model must lead to a 6×6 determinantal secular equation for the energy. The method used group theory is able to solve it easily. Slonczewski and Weiss found that the Lomer's work can be simplified greatly by a different choice of the location of the origin (Slonczewski & Weiss, 1958). A better tight-binding description of graphene was given by Saito et al. (Saito et al., 1998), which considers the nonfinite overlap between nearest neighbors, but includes only interactions between nearest neighbors. To understand the different levels of approximation, Reich et al. started from the most general form of the secular equation, the tight binding Hamiltonian, and the overlap matrix to calculate the band structure (Reich et al., 2002). But their work did not involve the effect of the non-nearest-neighbor interaction on the band structure. This work will be discussed in details in Section 2.

Because there is no energy gap, perfect graphene sheets are metallic. How open the gap of graphene? According to the quantum size effect, graphene nanoribbons maybe achieve this

goal. Early in 1996, Fujita et al. started to study the electronic structure of graphene ribbons (Fijita et al.,1996; Nakada et al., 1996) by the numerical method. For perfect graphene ribbons, the armchair shaped edge ribbons can be either semiconducting ($n=3m$ and $n=3m+1$, where m is an integer) or metallic ($n=3m+2$) depending on their widths. First-principles calculations show that the origin of the gaps for the armchair edge nanoribbons arises from both quantum confinement and the deformation caused by edge dangling bonds (Son et al., 2006; Rozhkov et al., 2009). In low-energy approximation, the analytical electronic states of the nanoribbons are studied based on the Dirac equation (Brey & Fertig, 2006). In 2007, Zheng et al. got an analytical expression of the electronic structure, including the boundary relaxation, for the armchair nanoribbon by the tight-binding approximation and hard-wall boundary condition, which only involves the nearest-neighbor hopping integrals (Zheng et al., 2007). In this chapter, we focus on the effects of the non-nearest-neighbor hopping integrals and atomic wave function overlap on the electronic structure, and on the competition between the non-neighbor interaction and edge deformation. The tight-binding energy dispersion relations of graphene nanoribbons, including up to third neighbors, are introduced in section 3. In Section 4, the competition of both is discussed. The stretching deformation of graphene ribbons based on the elastic theory is presented in last section.

2. The non-nearest-neighbor effect in graphene sheets

In this section the tight-binding method is used to study the band structure of the π electrons in graphene. Although this method is simple, it provides a lot of important information for understanding the π electronic band structure. The first tight-binding description for graphene was given by Wallace (Wallace, 1947). He considered nearest- and next-nearest-neighbor interaction for the graphene $2p_z$ orbitals, but neglected the overlap between wave functions centred at different atoms. To compensate for the lack of this work, the non-finite overlap between the basis functions was considered (Saito et al., 1998), but the interaction between nearest neighbors was taken only into account. A better tight-binding description including up to third-nearest neighbors for graphene was given by Reich et al. (Reich et al., 2002).

Let us now consider the band structure from the viewpoint of the tight-binding approximation. The structure of graphene is composed of two types of sublattices A and B as shown in Fig.1. If $\varphi(\boldsymbol{r})$ is the normalized orbital $2p_z$ wave function for an isolated carbon atom, then the wave function of graphene has the form

$$|\psi\rangle = C_A|\psi_A\rangle + C_B|\psi_B\rangle,\tag{1}$$

where

$$|\psi_A\rangle = \frac{1}{\sqrt{N}}\sum_A e^{i\boldsymbol{k}\cdot\boldsymbol{R}_A}\varphi(\boldsymbol{r}-\boldsymbol{R}_A),$$

and

$$|\psi_B\rangle = \frac{1}{\sqrt{N}}\sum_B e^{i\boldsymbol{k}\cdot\boldsymbol{R}_B}\varphi(\boldsymbol{r}-\boldsymbol{R}_B).\tag{2}$$

The first sum is taken over A and all the lattice points generated from it by primitive lattice translation; the second sum is similarly over the points generated from B. Here C_A and C_B are coefficients to be determined, R_A and R_B are the positions of atoms A and B, respectively, and N is the number of the unit cell in a graphene sheet.

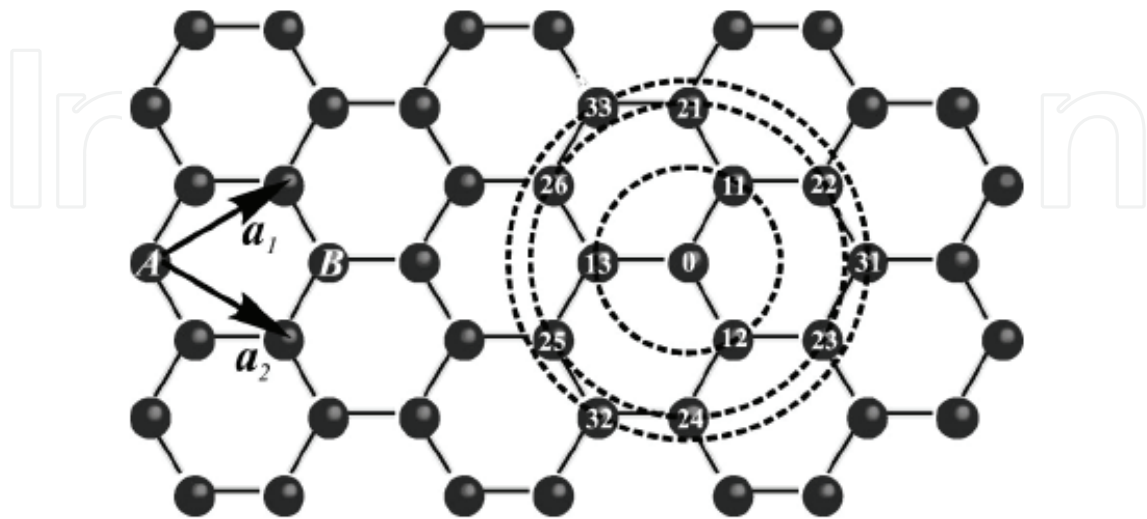Fig. 1. Structure of a graphene sheet, consisting of sublattices A and B. a_1 and a_2 are the unit-cell vectors of graphene with a lattice constant a = 0.246 nm. A carbon atom A_0 has three nearest neighbors B_{1i}, six next-nearest neighbors A_{2i}, and three second-nearest neighbors B_{3i}.(Reich et al., 2002)

Under the tight-binding approximation, the Hamiltonian of the perfect system is

$$H = \sum_i \varepsilon |i\rangle\langle i| - \sum_{(i,j)} \gamma_0 |i\rangle\langle j| - \sum_{((i,j))} \gamma_1 |i\rangle\langle j| - \sum_{(((i,j)))} \gamma_2 |i\rangle\langle j| , \qquad (3)$$

where (i,j), $((i,j))$, and $(((i,j)))$ denote the nearest, next-nearest, and third neighbors, respectively, ε is the self-energy of the site atom, and γ_0, γ_1, and γ_2 are the nearest-, next-nearest-, and third-neighbor hopping energies. Substituting Eq. (1) in

$$H|\psi\rangle = E|\psi\rangle , \qquad (4)$$

and carrying out a simple derivation and finishing, we obtain the secular equation

$$\begin{vmatrix} H_{AA}(\boldsymbol{k}) - E(\boldsymbol{k})S_{AA}(\boldsymbol{k}) & H_{AB}(\boldsymbol{k}) - E(\boldsymbol{k})S_{AB}(\boldsymbol{k}) \\ H^*_{AB}(\boldsymbol{k}) - E(\boldsymbol{k})S^*_{AB}(\boldsymbol{k}) & H_{AA}(\boldsymbol{k}) - E(\boldsymbol{k})S_{AA}(\boldsymbol{k}) \end{vmatrix} = 0 , \qquad (5)$$

where $E(\boldsymbol{k})$ are the electronic energy eigenvalues and $\boldsymbol{S}$ is the overlap matrix. In Eq.(5), we have made use of the equivalence of the A and B carbon atoms in the graphene sheet. The solution to Eq.(5) is

$$E_\pm(\boldsymbol{k}) = \frac{-(-2E_0 + E_1) \pm \sqrt{(-2E_0 + E_1)^2 - 4E_2 E_3}}{2E_3} , \qquad (6)$$

with

$$E_0 = H_{AA}S_{AA}, \quad E_1 = S_{AB}H_{AB}^* + H_{AB}S_{AB}^*,$$

$$E_2 = H_{AA}^2 - H_{AB}H_{AB}^*, \quad E_3 = S_{AA}^2 - S_{AB}S_{AB}^*. \tag{7}$$

The plus sign denotes the conduction band and the minus sign is the valence band. To calculate the Hamiltonian and overlap matrix elements, we derive the third-neighbor tight-binding description. We see from Fig.1 that a carbon atom A has three nearest neighbors B_{1i}, six next-nearest neighbors A_{2i}, and three second-nearest neighbors B_{3i}, all of which belong to the other sublattice.

For third-neighbor interaction the Hamiltonian matrix element H_{AA} can be written as

$$
\begin{aligned}
H_{AA} &= \langle \psi_A | H | \psi_A \rangle \\
&= \frac{1}{N} \sum_{R_A} \sum_{R'_A} e^{i k \cdot (R'_A - R_A)} \langle \varphi(r - R_A) | H | \varphi(r - R'_A) \rangle \\
&= \frac{1}{N} \sum_{R_A} \langle \varphi(r - R_A) | H | \varphi(r - R_A) \rangle \\
&\quad + \frac{1}{N} \sum_{R_A, R_{Ai}} e^{i k \cdot R_{Ai}} \langle \varphi(r - R_A) | H | \varphi(r - R_A - R_{Ai}) \rangle \\
&= \varepsilon + \frac{1}{N} \sum_{R_A} \gamma_1 \left\{ e^{i k \cdot R_{A1}} + e^{i k \cdot R_{A2}} + e^{i k \cdot R_{A3}} + e^{i k \cdot R_{A4}} + e^{i k \cdot R_{A5}} + e^{i k \cdot R_{A6}} \right\}
\end{aligned}
\tag{8}
$$

where R_{Ai} is the position vectors of six next-nearest neighbor atoms A_i with respect to atom A. Here ε is called the $2p$ orbital energy, or self-energy, of the site atom, which is given by

$$\varepsilon = \langle \varphi(r - R_A) | H | \varphi(r - R_A) \rangle, \tag{9}$$

and γ_1 is the next-nearest-neighbor hopping integral of π electrons and defined as follows

$$\gamma_1 = \langle \varphi(r - R_A) | H | \varphi(r - R_A - R_{Ai}) \rangle, \quad (i = 1,2,3,4,5,6). \tag{10}$$

In Eq.(8) the maximum contribution to the matrix element H_{AA} is the first term, which comes from the orbital energy of $R'_A = R_A$. The next order contribution to H_{AA} is the second term coming from terms of $R'_A = R_A + R_{Ai}$. The other order contribution to this matrix element is very small compared to the first term, which can be neglected. If we define the function

$$
\begin{aligned}
u(k) &= 2\cos k \cdot a_1 + 2\cos k \cdot a_2 + 2\cos k \cdot (a_1 - a_2) \\
&= 2\cos 2\pi k_1 a + 2\cos 2\pi k_2 a + 2\cos 2\pi a (k_1 - k_2),
\end{aligned}
\tag{11}
$$

where $k_i = k \cdot a_i / 2\pi$ are the components of a wave vector k in units of the reciprocal lattice vectors k_1 and k_2, and $a = |a_1| = |a_2| = 0.246$ nm is the lattice constant of graphene, then Eq.(8) can be rewritten as

$$H_{AA} = \varepsilon + \gamma_1 u(k). \tag{12}$$

Let us next calculate H_{AB}. For this, we shall consider interactions between nearest, and third neighbors in the lattice, the nearest and third neighbors of atoms of type A being always atoms of type B. Therefore, the matrix element H_{AB} is

$$
\begin{aligned}
H_{AB} &= \langle \psi_A | H | \psi_B \rangle \\
&= \frac{1}{N} \sum_{R_A} \sum_{R_B} e^{ik \cdot (R_B - R_A)} \langle \varphi(r - R_A) | H | \varphi(r - R_B) \rangle \\
&= \gamma_0 (e^{ik \cdot R_{B11}} + e^{ik \cdot R_{B12}} + e^{ik \cdot R_{B13}}) + \gamma_2 (e^{ik \cdot R_{B31}} + e^{ik \cdot R_{B32}} + e^{ik \cdot R_{B33}}),
\end{aligned}
\tag{13}
$$

where the hopping energies are given by

$$
\gamma_0 = \langle \varphi(r - R_A) | H | \varphi(r - R_A - R_{B1i}) \rangle \quad (i = 1,2,3),
\tag{14}
$$

$$
\gamma_2 = \langle \varphi(r - R_A) | H | \varphi(r - R_A - R_{B3i}) \rangle \quad (i = 1,2,3).
\tag{15}
$$

Here R_{B1i} and R_{B3i} are the vectors pointing from atom A to atoms B_{1i} and B_{3i}, respectively. Using the same treatment we can obtain the overlap matrix element

$$
\begin{aligned}
S_{AA} &= \langle \psi_A | \psi_A \rangle \\
&= \frac{1}{N} \sum_{R_A} \sum_{R'_A} e^{ik \cdot (R'_A - R_A)} \langle \varphi(r - R_A) | \varphi(r - R'_A) \rangle \\
&= 1 + \frac{1}{N} \sum_{R_A} \sum_i e^{ik \cdot R_{A2i}} \langle \varphi(r - R_A) | \varphi(r - R_A - R_{A2i}) \rangle \\
&= 1 + s_1 u(k)
\end{aligned}
\tag{16}
$$

with

$$
s_1 = \langle \varphi(r - R_A) | \varphi(r - R_A - R_{A2i}) \rangle \quad (i = 1,2,3,4,5,6),
\tag{17}
$$

where R_{A2i} are the vectors pointing from atom A to atoms A_{2i}, and s_1 is the overlap of atomic wave functions between next-nearest neighbors. Similarly, we have

$$
\begin{aligned}
S_{AB} &= \langle \psi_A | \psi_B \rangle \\
&= \frac{1}{N} \sum_{R_A} \sum_{R_B} e^{ik \cdot (R_B - R_A)} \langle \varphi(r - R_A) | \varphi(r - R_B) \rangle \\
&= s_0 (e^{ik \cdot R_{B11}} + e^{ik \cdot R_{B12}} + e^{ik \cdot R_{B13}}) + s_2 (e^{ik \cdot R_{B31}} + e^{ik \cdot R_{B32}} + e^{ik \cdot R_{B33}}),
\end{aligned}
\tag{18}
$$

where s_0 and s_2 are the overlap integrals between nearest, and third neighbors, which are given by

$$
s_0 = \langle \varphi(r - R_A) | \varphi(r - R_A - R_{B1i}) \rangle \quad (i = 1,2,3),
\tag{19}
$$

and

$$
s_2 = \langle \varphi(r - R_A) | \varphi(r - R_A - R_{B3i}) \rangle \quad (i = 1,2,3).
\tag{20}
$$

Substituting Eqs.(12), (13), (16), and (18) into Eq.(7) yields

$$E_0 = [\varepsilon + \gamma_1 u(\boldsymbol{k})][1 + s_1 u(\boldsymbol{k})] , \tag{21}$$

$$E_1 = 2s_0\gamma_0[3 + u(\boldsymbol{k})] + (s_0\gamma_2 + s_2\gamma_0)g(\boldsymbol{k}) + 2s_2\gamma_2[3 + u(2\boldsymbol{k})] , \tag{22}$$

$$E_2 = [\varepsilon + \gamma_1 u(\boldsymbol{k})]^2 - \gamma_0^2[3 + u(\boldsymbol{k})] - \gamma_0\gamma_2 g(\boldsymbol{k}) - \gamma_2^2[3 + u(2\boldsymbol{k})], \tag{23}$$

$$E_3 = [1 + s_1 u(\boldsymbol{k})]^2 - s_0^2[3 + u(\boldsymbol{k})] - s_0 s_2 g(\boldsymbol{k}) - s_2^2[3 + u(2\boldsymbol{k})] , \tag{24}$$

where

$$g(\boldsymbol{k}) = 2u(\boldsymbol{k}) + u(2k_1 - k_2, k_1 - 2k_2) .$$

Inserting E_0 to E_3 into Eq.(6) we can obtain the tight-binding energy dispersion relation in the third-neighbor approximation.

To give the numerical results of energy dispersion, we must know the values of the hopping energies and overlap integrals. We take the parameters $\varepsilon = -0.28$ eV, $\gamma_0 = -2.97$ eV, $\gamma_1 = -0.073$ eV, $\gamma_2 = -0.33$ eV, $s_0 = 0.073$, $s_1 = 0.018$, and $s_2 = 0.026$ (Reich et al., 2002). The computed results for some high-symmetry points ($K\Gamma M$) are shown in Fig. 2, where the solid line denotes the nearest-neighbor result, the dashed line represents the next-nearest-neighbor, and the dotted line is the third-neighbor. It is clear that the next-nearest-neighbor hopping integrals and overlap between atomic wave functions will play an important role on the band width at Γ point, which can largely reduce the bandwidth, and the third-neighbor interaction can slightly enhance the bandwidth. But the role of both is just opposite for M point. It is worth pointing out that when we take only into account the nearest neighbor hopping integral and let both the overlap s_0 and the site energy ε be zero, the energy bands are symmetric with respect to the Fermi level. The nearest neighbor result in Fig. 2 is to include the overlap s_0, so the energy bands become asymmetric, leading to the
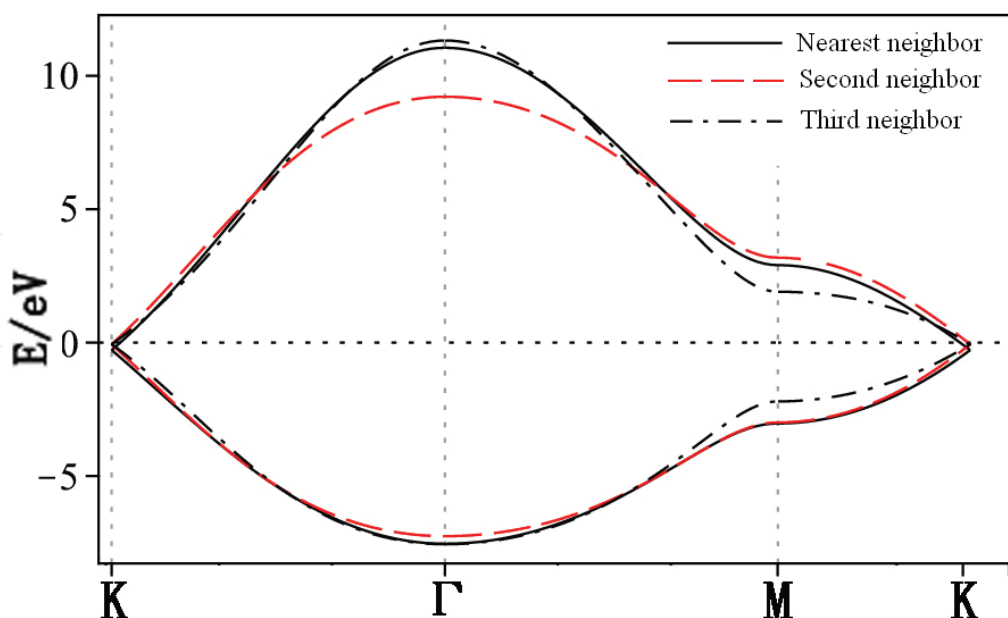

Fig. 2. Tight-binding energy bands of graphene for high-symmetry points. The solid line denotes the nearest neighbor, the dashed line represents the next-nearest neighbor, and the dotted line is the third neighbor.

Fermi level down slightly. This means that the overlap integral is important for the band structure. Hence, the non-nearest neighbor hopping and overlap integral need to be considered in calculations of the energy band. Since there is no energy gap at K point (Dirac point), the graphene sheet is metallic.

3. The non-nearest-neighbor effect in graphene nanoribbons

3.1 Armchair nanoribbons

As mentioned in Section 2, for a graphene sheet there are no energy gaps at the Dirac points. How to open the energy gaps of graphene? One method is to deduce the size of graphene and let it become a narrow ribbon, compared to the length of the ribbon. From this, the band gaps will change with their widths (Son et al., 2006), and the more narrow the width is, the larger the gap. Another effective approach is to change the bond length of graphene by exerting a strain force. Besides, we can also open the gap by using absorption atoms on graphene or doping impurity in. For an armchair ribbon, the analytical solution of electronic dispersion has been given based on the tight-binding approach, but the dispersion obtained is in the framework of the nearest-neighbor interaction (Zheng et al, 2007). In this section we only discuss the electronic dispersion of perfect graphene nanoribbons without any edge deformation within the tight-binding approximation and the third-neighbor interaction is taken into account.

We choose the ribbon to be macroscopically large along the x direction but finite in the y direction, which leads to a graphene nanoribbon with armchair edges. Since the ribbon is very long compared to its width and has the translational symmetry along the x direction, we can choose the plane-wave basis along the x direction and take the stationary wave in the y direction because the electronic bahavior is limited to the space between two edges. The structure of armchair nanoribbons consists of two types of sublattices A and B, and the unit cell contains n A-type carbon atoms and n B-type atoms as illustrated in Fig.3.
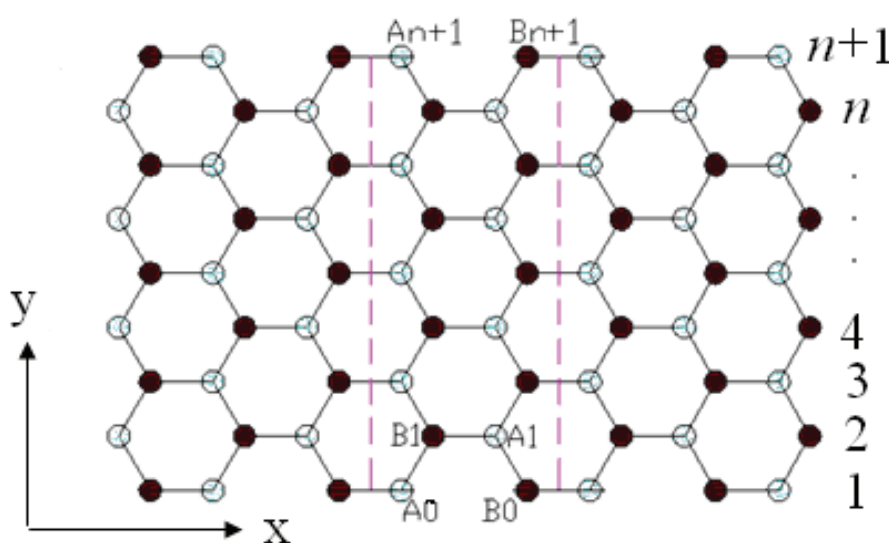

Fig. 3. Structure of an armchair graphene ribbon with sublattices A (empty) and B (solid). The ribbon width is denoted by numbers n. Every unit cell has n numbers of A and B sublattices. Assume that the edges of the ribbon are a hard wall.

Within the tight-binding approximation, the wave functions of A and B sublattices can be written as

$$|\psi_A\rangle = \frac{1}{N_A} \sum_{j=1}^{n} \sum_{x_{A_j}} e^{ik_x x_{A_j}} \phi_A(j) |\varphi(\boldsymbol{r} - \boldsymbol{R}_{A_j})\rangle, \qquad (25)$$

$$|\psi_B\rangle = \frac{1}{N_B} \sum_{j=1}^{n} \sum_{x_{B_j}} e^{ik_x x_{B_j}} \phi_B(j) |\varphi(\boldsymbol{r} - \boldsymbol{R}_{B_j})\rangle, \qquad (26)$$

where N_A and N_B are the normalized coefficients, $\phi_A(j)$ and $\phi_B(j)$ are the components for A and B sublattices in the y direction and satisfy the following hard-wall boundary conditions

$$\phi_A(0) = \phi_B(0) = 0,$$

$$\phi_A(n+1) = \phi_B(n+1) = 0. \qquad (27)$$

Assume that the stationary wave has the form

$$\phi_A(j) = \phi_B(j) = \sin\left(\frac{1}{2}\sqrt{3}ak_y j\right), \ (j = 1, 2, \cdots, n) \qquad (28)$$

leading to a discretized wave vector in the y direction

$$k_y(q) = \frac{2\pi q}{\sqrt{3}a(n+1)}, \ (q = 1, 2, \cdots, n). \qquad (29)$$

To find out the normalized coefficients in Eqs.(25) and (26), we introduce the normalization condition

$$\langle \psi_A | \psi_A \rangle = \langle \psi_B | \psi_B \rangle = 1, \qquad (30)$$

from which, we get

$$N_A = N_B = \sqrt{N_x(n+1)/2},$$

where N_x is the number of unit cells along the x direction. Therefore, the total wave function of the graphene ribbon can be written as

$$\begin{aligned}|\psi\rangle &= C_A |\psi_A\rangle + C_B |\psi_B\rangle \\ &= C_A \sqrt{\frac{2}{N_x(n+1)}} \sum_{j=1}^{n} \sum_{x_{A_j}} e^{ik_x x_{A_j}} \sin\left(j\sqrt{3}k_y a/2\right) |\varphi(\boldsymbol{r} - \boldsymbol{R}_{A_j})\rangle \\ &\quad + C_B \sqrt{\frac{2}{N_x(n+1)}} \sum_{j=1}^{n} \sum_{x_{B_j}} e^{ik_x x_{B_j}} \sin\left(j\sqrt{3}k_y a/2\right) |\varphi(\boldsymbol{r} - \boldsymbol{R}_{B_j})\rangle.\end{aligned} \qquad (31)$$

Substituting Eqs.(3) and (31) into the Schrodinger equation leads to an energy dispersion relation of the form

$$E_{\pm}(k_x, q) = \frac{-(2E_0 + E_1) \pm \sqrt{(-2E_0 + E_1)^2 - 4E_2 E_3}}{2E_3} ,\qquad (32)$$

where

$$E_0(k_x, q) = \{\varepsilon + \gamma_1[f(k_x, q) - 3]\}\{[1 + s_1[f(k_x, q) - 3]\} ,\qquad (33)$$

$$E_1(k_x, q) = 2s_0\gamma_0 f(k_x, q) + (s_0\gamma_2 + s_2\gamma_0)g(k_x, q) + 2s_2\gamma_2 h(k_x, q) ,\qquad (34)$$

$$E_2(k_x, q) = \{\varepsilon + \gamma_1[f(k_x, q) - 3]\}^2 - \gamma_0^2 f(k_x, q) - \gamma_0\gamma_2 g(k_x, q) - \gamma_2^2 h(k_x, q) ,\qquad (35)$$

$$E_3(k_x, q) = \{1 + s_1[f(k_x, q) - 3]\}^2 - s_0^2 f(k_x, q) - s_0 s_2 g(k_x, q) - s_2^2 h(k_x, q) ,\qquad (36)$$

and

$$f(k_x, q) = 1 + 4\cos\left(\frac{q\pi}{n+1}\right)\cos\left(\frac{3k_x a}{2}\right) + 4\cos^2\left(\frac{q\pi}{n+1}\right) ,$$

$$h(k_x, q) = 1 + 4\cos\left(\frac{2q\pi}{n+1}\right)\cos(3k_x a) + 4\cos^2\left(\frac{2q\pi}{n+1}\right) ,$$

$$g(k_x, q) = 2f(k_x, q) + 2\cos\left(\frac{3k_x a}{2} + \frac{3q\pi}{n+1}\right) + 2\cos\left(\frac{3k_x a}{2} - \frac{3q\pi}{n+1}\right) + 2\cos(3k_x a) - 6 .$$

The electronic dispersion given by Eq. (32), in form, is exactly the same as that found for a graphene sheet, but both have the difference in nature (Jin et al., 2009). The region $-\pi/3 \leq k_x a \leq \pi/3$ is within the first Brillouin zone. These results are valid for various energy ranges.

Since the electronic structure of perfect armchair graphene nanoribbons depends strongly on the width of the ribbon, the system, for instance, is metallic when $n=3m+2$ (m is an integer) and is insulating otherwise. To give a graph of energy bands, we still use the same parameter values as taken in a graphene sheet. The electronic energy bands of the armchair nanoribbons with three different widths are plotted in Fig.4, where (a) is $n=3m=6$, (b) $n=3m+1=7$, and (c) $n=3m+2=8$. Labels (1), (2), and (3) denote the nearest, next-nearest, and third neighbors, respectively. As $n = 6$ and $n = 7$, the armchair ribbons appear insulating. Fig.4 shows that the next-nearest-neighbor hopping and overlap integral would give rise to change of the energy band width. This is because the energy levels of the conduction band top are squeezed, which correspond to the stationary waves with small q values. The third neighbors not only affect the energy gaps, such as $n=6$ and $n=7$, but also the band widths. The influence on the band width mainly is because the bands related to the standing waves with small q values in conduction and valence band produce a larger bend and this effect was particularly evident when $n=7,8$. However, the effect on the energy gaps is because the bands corresponding to larger q go down slightly. It is worth noting that when $n = 7$, there is a flat conduction or valence band, taking not into account the third neighbors, which corresponds to the quantum number $q=(n+1)/2$. Such a flat band is independent of wave vector k_x and in general exists only when n is equal to odd. As for $n = 8$, the lowest

conduction band and the upmost valence band touch at Dirac point, which leads to the metallic behavior of the armchair ribbon.
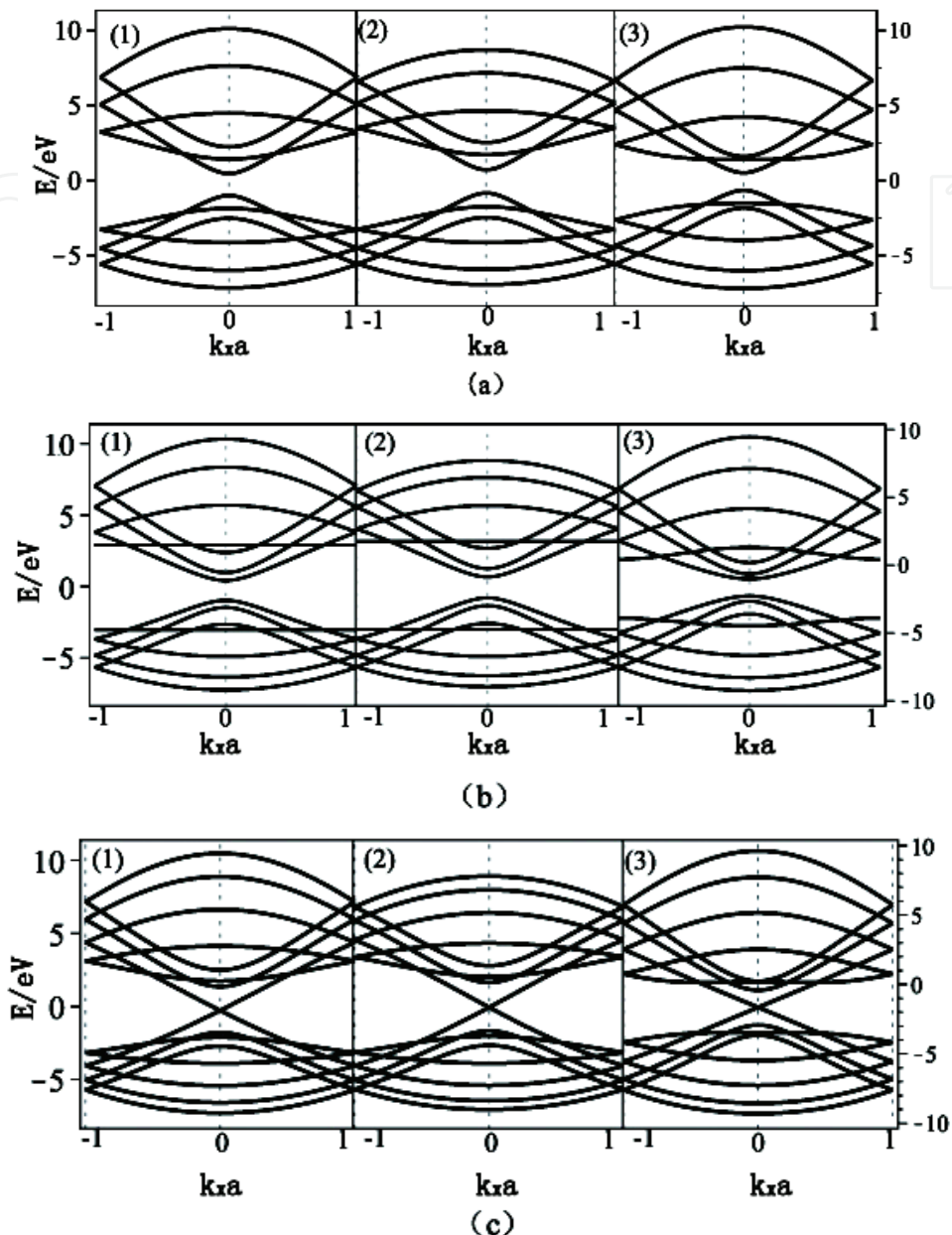

Fig. 4. Energy bands of perfect armchair graphene nanoribbons with widths (a) *n*=6, (b) *n*=7, and (c) *n*=8. Labels (1), (2), and (3) represent the nearest, next-nearest, and third neighbors, respectively.

3.2 Zigzag nanoribbons

The spectrum of graphene nanoribbons depends on the nature of their edges: zigzag or armchair. In Fig. 5, we show a honeycomb lattice having zigzag edges along the *x* direction and armchair edges along the *y* direction, where the solid cycles denote the sublattice *A* and the empty is *B*. If we choose the ribbon to be infinite in the *x* direction, we produce a graphene nanoribbon with zigzag edges. It is interesting to note that the atoms at each edge are of the same sublattice (*B* on the top edge of Fig. 5 and *A* on the bottom).
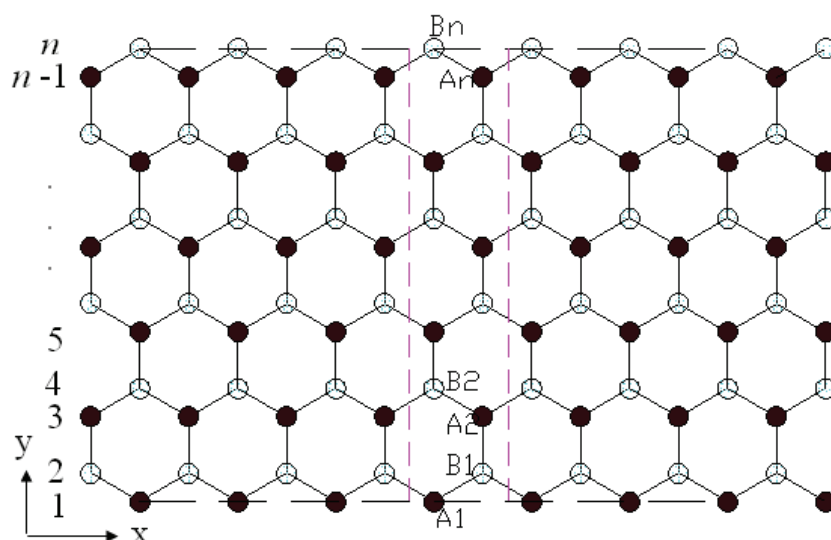
Fig. 5. The structure of a zigzag graphene nanoribbon, having the translational symmetry along the *x* direction. Atoms enclosed in the vertical rectangle represent the unit cell. *n* is the row number of atoms. The solid cycles denote the sublattice *A* and the empty is *B*.

We now calculate the electronic energy bands of the zigzag ribbon as shown in Fig.5 by using the tight-binding approach including up to third-nearest neighbors. To do this, let us label the sublattices *A* and *B* with number, respectively, and let A_1, A_2,…, A_n correspond to odd labels 1,3,5,…,2n-1 and B_1, B_2,…, B_n to even labels 2,4,…,2n. From this, the Hamiltonian becomes a 2n×2n matrix, which is given by

$$
\mathbf{H} = \begin{bmatrix}
f_2 & f_0 & f_1 & \gamma_2 & 0 & 0 & \cdots & \cdots \\
f_0 & f_2 & f_3 & f_1 & 0 & 0 & \cdots & \cdots \\
f_1 & f_3 & f_2 & f_0 & f_1 & \gamma_2 & \cdots & \cdots \\
\gamma_2 & f_1 & f_0 & f_2 & f_3 & f_1 & \cdots & \cdots \\
0 & 0 & f_1 & f_3 & f_2 & f_0 & f_1 & \gamma_2 \\
0 & 0 & \gamma_2 & f_1 & f_0 & f_2 & f_3 & f_1 \\
\cdots & \cdots & \cdots & \cdots & \cdots & \cdots & \cdots & \cdots
\end{bmatrix}, \tag{37}
$$

where f_0, f_1, f_2, and f_3 are the Hamiltonian matrix elements, which are given by

$$
f_0 = \left\langle \psi_j \middle| H \middle| \psi_i \right\rangle = 2\gamma_0 \cos\left(\frac{\sqrt{3}k_x a}{2}\right) \qquad (j = i-1), \tag{38}
$$

$$
f_1 = \left\langle \psi_j \middle| H \middle| \psi_i \right\rangle = 2\gamma_1 \cos\left(\frac{\sqrt{3}k_x a}{2}\right) \qquad (j = i \pm 2), \tag{39}
$$

$$
f_2 = \left\langle \psi_j \middle| H \middle| \psi_i \right\rangle = \varepsilon + 2\gamma_1 \cos\left(\sqrt{3}k_x a\right) \qquad (j = i), \tag{40}
$$

$$
f_3 = \left\langle \psi_j \middle| H \middle| \psi_i \right\rangle = \gamma_0 + 2\gamma_2 \cos\left(\sqrt{3}k_x a\right) \qquad (j = i+1). \tag{41}
$$

γ_0, γ_1, and γ_2 are the nearest-, next-nearest-, and third-neighbor electronic hopping amplitudes, respectively. Similarly, the overlap matrix S can be written as

$$S = \begin{bmatrix} g_2 & g_0 & g_1 & s_2 & 0 & 0 & ... & ... \\ g_0 & g_2 & g_3 & g_1 & 0 & 0 & ... & ... \\ g_1 & g_3 & g_2 & g_0 & g_1 & s_2 & ... & ... \\ s_2 & g_1 & g_0 & g_2 & g_3 & g_1 & ... & ... \\ 0 & 0 & g_1 & g_3 & g_2 & g_0 & g_1 & s_2 \\ 0 & 0 & s_2 & g_1 & g_0 & g_2 & g_3 & g_1 \\ ... & ... & ... & ... & ... & ... & ... & ... \end{bmatrix},$$ (42)

where

$$g_0 = \langle \psi_j | \psi_i \rangle = 2s_0 \cos\left(\frac{\sqrt{3}k_x a}{2}\right) \quad (j = i-1),$$ (43)

$$g_1 = \langle \psi_j | \psi_i \rangle = 2s_1 \cos\left(\frac{\sqrt{3}k_x a}{2}\right) \quad (j = i \pm 2),$$ (44)

$$g_2 = \langle \psi_j | \psi_i \rangle = 1 + 2s_1 \cos\left(\sqrt{3}k_x a\right) \quad (j = i),$$ (45)

$$g_3 = \langle \psi_j | \psi_i \rangle = s_0 + 2s_2 \cos\left(\sqrt{3}k_x a\right) \quad (j = i+1).$$ (46)

Here s_0, s_1, and s_2 are the nearest-, next-nearest-, and third-neighbor overlap integrals between the $2p_z$ orbitals, respectively. Substituting Eqs.(36) and (37) into the following secular equation

$$\det\left[\mathbf{H} - E\mathbf{S}\right] = 0,$$ (47)

we can obtain all n eigenvalues of E_i (k_x) (i=1,...,2n) for a given wave vector k_x. The electronic dispersion relations (or energy bands) of zigzag nanoribbons are shown in Fig. 6.
In order to conveniently compare with the third-neighbor result, we also give the nearest- and next-nearest-neighbor electronic energy bands together with it. In Fig. 6(a) and (b), the left is the nearest-neighbor result, the middle is the next-nearest-neighbor, and the right is the third-neighbor for the ribbon widths n=4 and n=10. We see from Fig.6 that the zigzag graphene nanoribbons are metallic and the energy bands are wide (more than 10eV), and the spacing between the energy bands is decreased as increasing of the width n. When the nearest neighbor interaction is taken only into account, the energy band structure is symmetrical (see Fig.6 (1)). But the next-nearest-neighbor hopping and overlap can make the energy bands become nonsymmetrical, i.e. the conduction band becomes narrowed and the valence band is widened. It is obvious that the top of the conduction band is pressed downward and the bottom of the valence band is pulled downward. However, the effect of the third neighbors on the band structure is the same as that of the next-nearest neighbors, but the latter is stronger than the former.
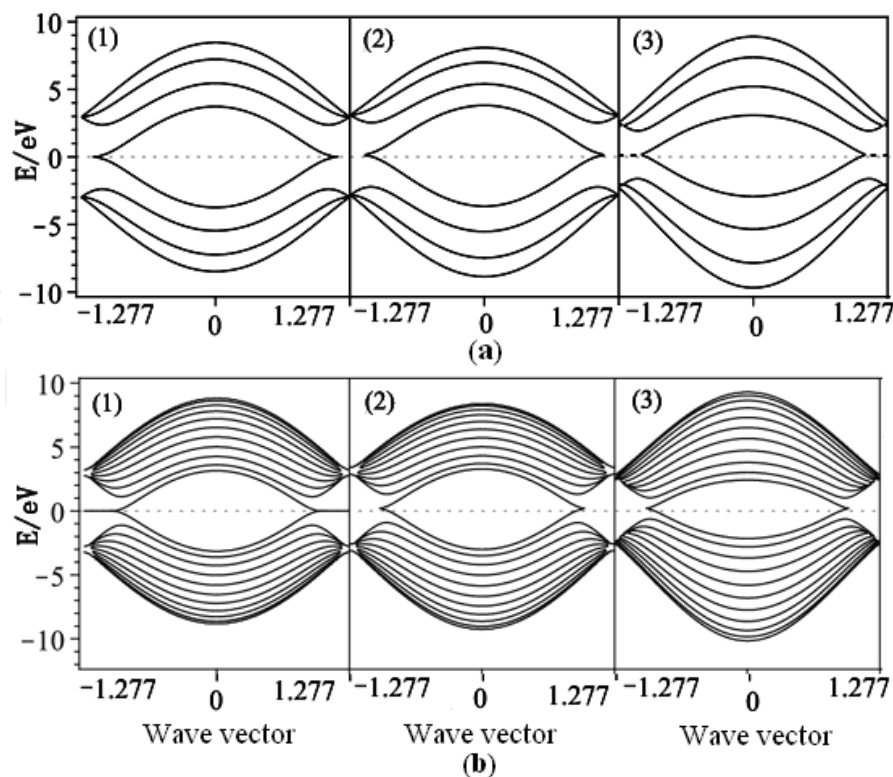
Fig. 6. Energy bands of zigzag nanoribbons with widths (a) $n=4$ and (b) $n=10$. Labels (1), (2), and (3) refer to the nearest, next-nearest, and third neighbors, respectively.

On the other hand, we see that the highest valence band state and the lowest conduction band state for the zigzag ribbons are always degenerate at $k_x = 1.277$. A pair of almost flat bands appears within the region of $0.851 \leq |k_x| \leq 1.277$ where the bands sit in the very vicinity of the Fermi level. This phenomenon arises only in the nearest neighbor result and does not occur in the non-nearest neighbor case. The degeneracy of the center bands at $k_x = 1.277$ does not originate from the intrinsic band structure, and the corresponding wave functions are completely localized on the edge sites (Nakada et al., 1996).

Based on the above discussion, we conclude that the effect of the third-neighbor terms on the energy band of the zigzag ribbon is large compared to that of the next-nearest-neighbor terms. Therefore, it is important to include the third neighbors when we calculate the bands. This is because the distance between the next-neighbor carbon atoms is very close to that between the third-neighbor atoms.

4. Competition between the non-neighbor interaction and edge deformation

4.1 Energy gaps in armchair nanoribbons

We now discuss the change of the energy gaps in armchair graphene nanoribbons. The results of first-principles calculations (Son et al., 2006) show that the differences among three widths ($n=3m$, $n=3m+1$, and $n=3m+2$) are quite apparent.

Our aim is to take into account the non-neighbor hopping integral and overlap and to understand their contribution to the band gap. To do this, we need to derive the formulas of the band gaps from Eq. (31). After a simple derivation, we easily obtain the following band gap formulas (Jin et al., 2009)

$$\Delta^0 = -\frac{2\sqrt{(-\gamma_0 + \varepsilon s_0)^2 f}}{s_0^2 f - 1}, \tag{48}$$

$$\Delta^1 = -\frac{2\sqrt{f(\gamma_0 f s_1 + 3\gamma_1 s_0 - \varepsilon s_0 - f\gamma_1 s_0 - 3\gamma_0 s_1 + \gamma_0)^2 f}}{s_1^2 f^2 - 6 f s_1^2 + 2 f s_1 + 9 s_1^2 - 6 s_1 + 1 - s_0^2 f}, \tag{49}$$

$$\Delta^2 = \frac{\sqrt{4 u_1^2 u_2^2 - 4 u_1 u_2 u_5 + u_5 - 4(u_1^2 - f\gamma_0^2 - \gamma_0\gamma_2 g - \gamma_2^2 h)(u_2^2 - u_3)}}{(u_2^2 - u_3)}, \tag{50}$$
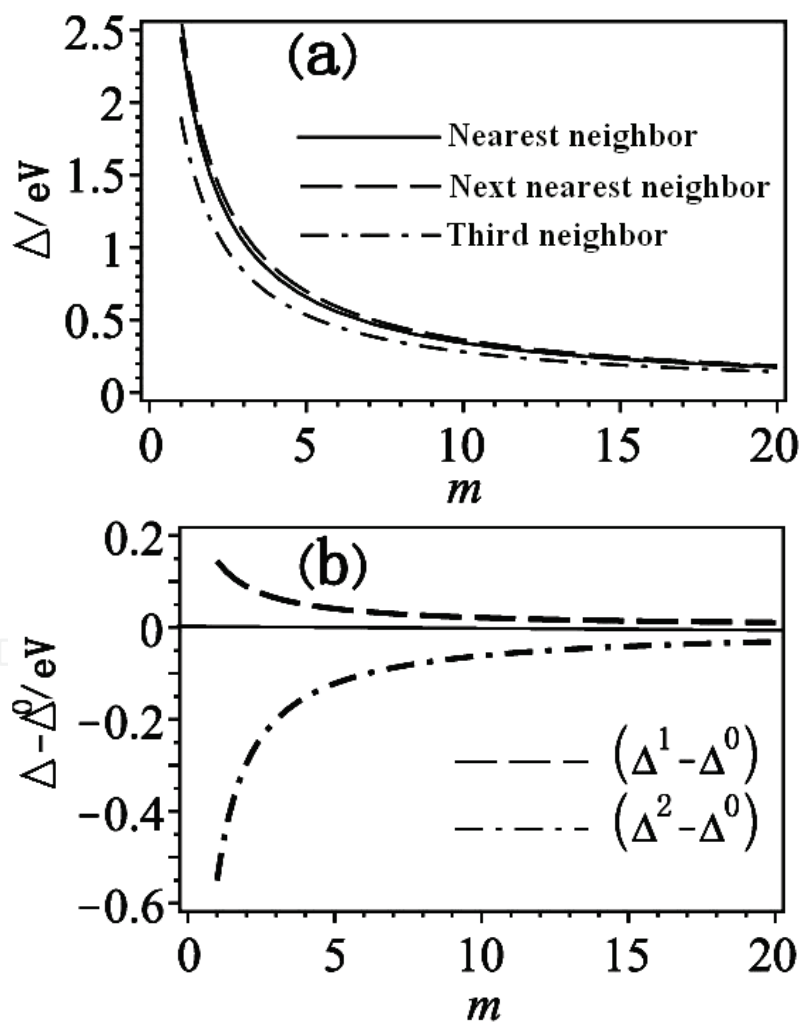
where

$$u_1 = \varepsilon + \gamma_1(f - 3),$$

Fig. 7. The variation of band gaps of armchair graphene nanoribbons for $n=3m$ as a function of width m. (a) Band gap curves for the nearest, next nearest, and third neighbors. (b) Band gap differences between the nearest and next nearest, and third neighbors.

$$u_2 = 1 + s_1(f - 3),$$

$$u_3 = s_0^2 f + s_0 s_2 g + s_2^2 h,$$

$$u_4 = (s_0 \gamma_2 + s_2 \gamma_0) g,$$

$$u_5 = 2 s_0 \gamma_0 f + u_4 + 2 s_2 \gamma_2 h.$$

Here Δ^0, Δ^1, and Δ^2 represent the band gaps of the nearest-, next-nearest-, and third-neighbor interaction, respectively. Quantities f, h, and g have been defined in Section 3. Since f, h, and g depend on the ribbon width n, the different width has the different band gap.

In order to illustrate the problem, we take $n=3m$ as an example to discuss the change of the gap with width. The results are summarized as function of width m, as shown in Fig.7, where the energy gap differences between the nearest and next-nearest neighbors and third neighbors are given together with. If we only consider the second-nearest-neighbor hopping and overlap, the difference between the nearest and next nearest neighbors is small for large m, but larger for small m. However, when we account to third neighbors, their contribution to the energy gap is large compared to that of the second neighbor, especially for small m.

4.2 Effect of the edge deformation on the energy gap

Because every carbon atom on the edge has one dangling bond unsaturated, the edge atoms of armchair nanoribbons are passivated by hydrogen atoms in general so that the σ bonds between hydrogen and carbon and the on-site energies of the carbons at the edges would be different from those in the middle of the ribbon. The bonding distances and angles between carbon atoms at the edges are also expected to change dramatically, which leads to considerable variations of electronic structure, especially within the low-energy range (Son et al., 2006). The bond lengths between carbon atoms at the edges are predicted to vary about 3-4% when hydrogenerated. Correspondingly, the hopping integral increases about 12% extracted from the analytical tight-binding expression (Son et al., 2006; Porezag et al., 1995).

To see the consequence of such effects more clearly, we introduce a simpler edge-deformed model, in which the Hamiltonian of the ribbon with deformation on the edge can be written as

$$H = \sum_i \varepsilon_i |i\rangle\langle i| - \sum_{(i,j)} (\gamma_0 + \delta\gamma_{0ij}) |i\rangle\langle j| - \sum_{((i,j))} (\gamma_1 + \delta\gamma_{1ij}) |i\rangle\langle j| - \sum_{(((i,j)))} (\gamma_2 + \delta\gamma_{2ij}) |i\rangle\langle j|. \quad (51)$$

As mentioned above, the variation of the next-nearest and third neighbor hopping integrals can be neglected for smaller deformation, i.e., $\delta\gamma_{1ij} = \delta\gamma_{2ij} = 0$. Let the variation of the hopping integral and the on-site energy of the ith carbon atom be $\delta\gamma_{0ij}$ and ε_i, respectively. Therefore, Eq.(51) cab be rewritten as

$$H = H_{0i} + H_i, \quad (52)$$

where

$$H_{0i} = \sum_i \varepsilon_i |i\rangle\langle i| - \sum_{(i,j)} \gamma_0 |i\rangle\langle j| - \sum_{((i,j))} \gamma_1 |i\rangle\langle j| - \sum_{(((i,j)))} \gamma_2 |i\rangle\langle j|, \quad (53)$$

$$H_i = -\sum_{(i,j)} \delta\gamma_{0ij} |i\rangle\langle j| . \tag{54}$$

The energy dispersion relation corresponding to the Hamiltonian H_{0i} still is the same as Eq.(32) in form, where ε is replaced by ε_i . For convenience, we rewrite Eq.(32) as follows

$$E_\pm^0(k_x, q) = \alpha \pm |\lambda| , \tag{55}$$

where α and λ are dependent of the parameters ε_i, γ_0, s_0, γ_1, s_1, and so on. Since H_i is small compared to H_{0i}, we can solve Eq.(52) by using the perturbation approach. Thus, a new dispersion relation is

$$E_\pm(k_x, q) = \beta \pm |\lambda + \delta\lambda| , \tag{56}$$

where β is the energy shift originating from the variation of the on-site energy and $\delta\lambda$ is the shift originating in the hopping integral variation. If the nearest neighbor interaction is involved only (Zheng et al., 2007), then β and $\delta\lambda$ are given by

$$\beta = \frac{2}{n+1} \sum_{i=1}^{n} \varepsilon_i \sin^2\left(\frac{q\pi}{n+1}i\right), \tag{57}$$

$$\delta\lambda = -\frac{2}{n+1} \sum_{i=1}^{n} \left[\delta\gamma_{0A(i)B(i)} \sin^2\left(\frac{q\pi}{n+1}i\right) e^{-ik_x a} \right.$$
$$+ \delta\gamma_{0A(i)B(i-1)} \sin\left(\frac{q\pi}{n+1}i\right) \sin\left(\frac{q\pi}{n+1}(i-1)\right) e^{ik_x a/2}$$
$$\left. + \delta\gamma_{0A(i)B(i+1)} \sin\left(\frac{q\pi}{n+1}i\right) \sin\left(\frac{q\pi}{n+1}(i+1)\right) e^{ik_x a/2} \right] \tag{58}$$

These results are valid for small edge deformations, atoms or molecules attached to edge carbon atoms. As long as given the deformation distribution function, we can obtain the energy dispersion relation of the edge deformation.

Assume that the deformation is very small and localized along two edges (Son et al., 2006), from Eqs.(55) and (56), we can obtain the differences between the energy gaps to the first order in $\delta\gamma_0$ and ε for different width ribbons as follows(Son et al., 2006; Zheng et al., 2007)

$$\Delta_{e3m} = \Delta_{3m} - \Delta_{3m}^0 = -\frac{8\delta\gamma_0}{3m+1} \sin^2\frac{m\pi}{3m+1} , \tag{59}$$

$$\Delta_{e3m+1} = \Delta_{3m+1} - \Delta_{3m+1}^0 = \frac{8\delta\gamma_0}{3m+2} \sin^2\frac{(m+1)\pi}{3m+2} , \tag{60}$$

$$\Delta_{e3m+2} = \Delta_{3m+2} - \Delta_{3m+2}^0 = \frac{2\delta\gamma_0}{m+1} . \tag{61}$$
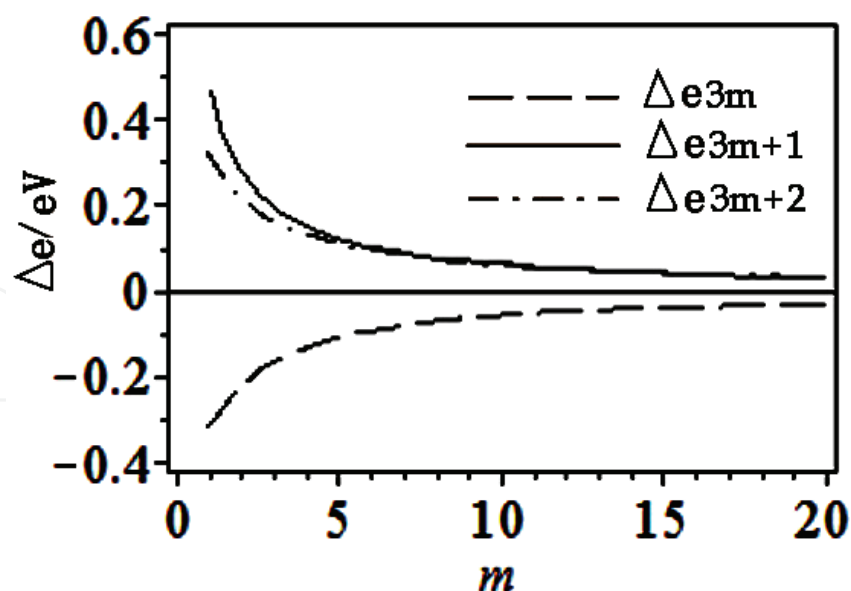
Fig. 8. The energy gap differences before and after deformation for armchair graphene ribbons. Solid, dashed, and dotted lines are the results of $n=3m+1$, $n=3m$, and $n=3m+2$, respectively.

Here the energy gap refers to the difference between the lowest conduction band and the highest valence band. Δ^0_{3m}, Δ^0_{3m+1}, and Δ^0_{3m+2} are the energy gaps of non-deformed ribbons. This result shows that all armchair graphene ribbons with edge deformation have nonzero energy gaps.

For smaller deformation, we set the hopping integral change $\delta\gamma_0/\gamma_0 = 0.12$ (Son et al., 2006). A graph of the gap difference vs. width m is shown in Fig.8. This implies that the 12% increase of the hopping integrals between carbon atoms at the edges opens the gaps of the $(3m+2)$ armchair ribbons and decreases (increases) the gaps of $3m$-armchair ribbons ($(3m+1)$-armchair ribbons). In order to facilitate comparison, we take $n=3m$ as an example. By comparing Fig.8 with Fig.7 (b), we see that the next-nearest neighbor effect is able to make the gap increase slightly with respect to the nearest neighbor case and the third-neighbor interaction would lead to decrease of the gap, and the smaller edge deformation would reduce the gap. Therefore, the competition results of both are that the effect of the boundary relaxation opposes the change of the next-nearest-neighbor interaction and strengthens the change of the third-neighbor interaction. The $n=3m+1$ situation is just opposite to the $n=3m$. For $n=3m+2$, the non-neighbor interaction does not change the gap and keeps this zero gap unchanged. Hence, there is no competition between the both. In fact, the edge deformation would have a penetration depth (Zheng et al., 2007). Since the depth is very small, our conclusions obtained above still are valid for this case.

5. Stretching deformation of graphene ribbons

In this section, we discuss the deformation of graphene due to an external force and effect of the deformation on the band gap. Assume that the length L of a graphene sheet is long compared to its width W, i.e. $L > W$, a wider ribbon satisfying translational symmetry in the length and width directions, and the force between carbon atoms satisfies Hook's law. We exert a tension force on the two edges of the graphene, as illustrated in Fig.9.
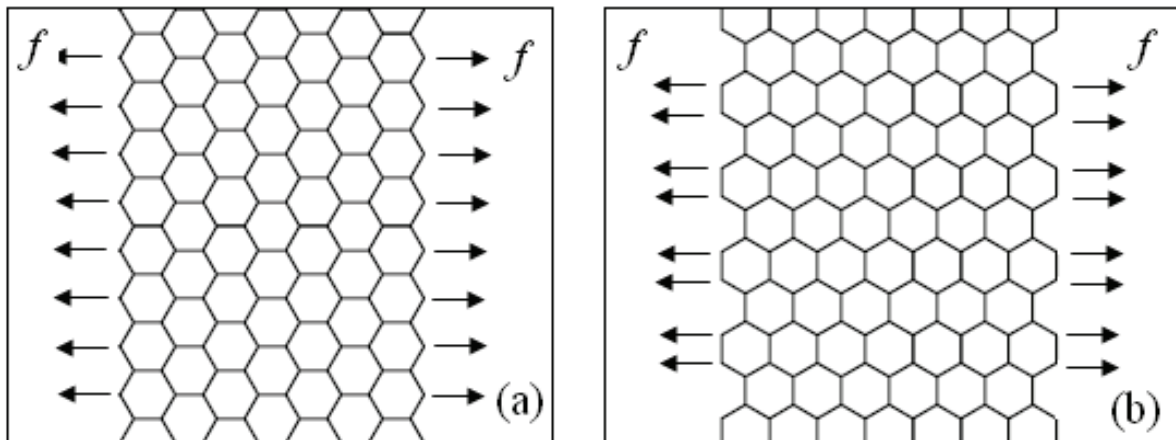
Fig. 9. Force on wider graphene ribbons with (a) zigzag and (b) armchair edges.

Let the force on each atom and lattice spring constant be f and k, respectively. The bond lengths and angles will change with the force and thereby lead to the change of hopping integrals, which causes the variation or opening of the energy gap. For zigzag edge ribbons, when an external force is much less than the stationary spring force between two neighbor atoms, the relation between the force f on each atom and bond half-angle α can be obtained

$$f_N = \frac{f}{kd_0} = \sqrt{3}\cot\alpha - 2\cos\alpha \tag{62}$$

Here d_0 is the original bond length, f_N is the dimensionless force on each atom. For small deformation, the bond half-angle is given by

$$\alpha = \frac{\pi}{3} + \frac{\sqrt{3}}{6}\left[(1+f_N) - \sqrt{1 + 14f_N + f_N^2}\right]. \tag{63}$$

Based on elastic mechanics, the deformed bond lengths are written as

$$d_1 = d_0(1 + f_N),$$

$$d_2 = d_3 = d_0\frac{\sqrt{3}}{2}\left/\sin\left(\frac{\pi}{3} + \frac{\sqrt{3}}{6}\left[(1+f_N) - \sqrt{1 + 14f_N + f_N^2}\right]\right)\right. . \tag{64}$$

Here d_1 is the bond length parallel to the direction of force f. Similarly, for armchair edge ribbons, we have

$$d_1' = d_0(1 - \frac{1}{6}f_N),$$

$$d_2' = d_3' = \frac{d_0}{2}\left/\cos\left(\frac{\pi}{3} - \frac{1}{2}\left[(\sqrt{3} + 2f_N) - \sqrt{(\sqrt{3} + 2f_N)^2 + 8f_N/\sqrt{3}}\right]\right)\right. . \tag{65}$$
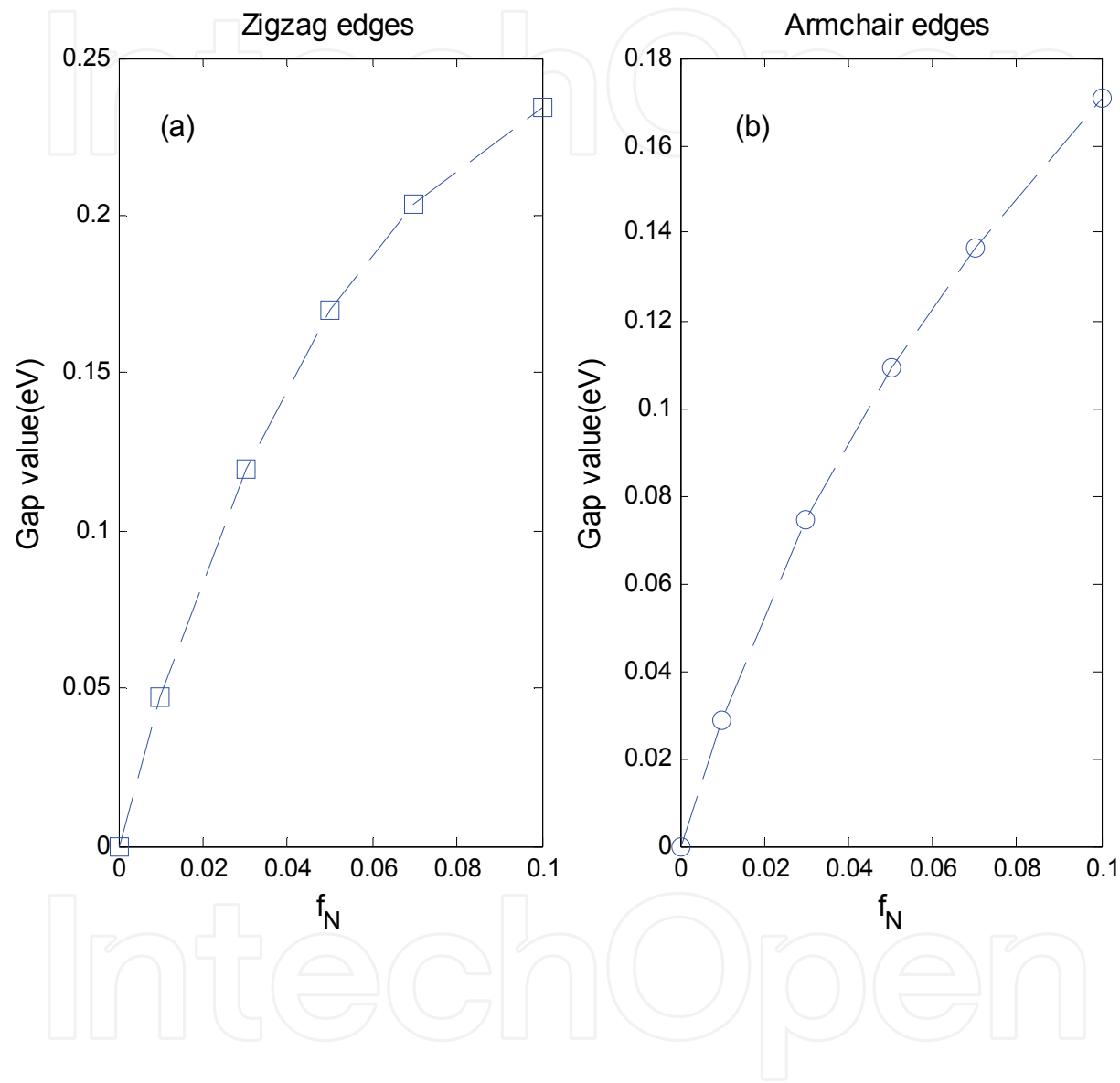
Fig. 10. Energy gaps of wider graphene ribbons with (a) zigzag and (b) armchair edges at K points as function of the dimensionless tensile force f_N.

Here d_1' is the bond length perpendicular to the direction of force f. To calculate hopping integrals, we choose the hydrogen-like atom wave functions as $2p_z$ orbitals, which is given by

$$\varphi(\boldsymbol{r}) = \sqrt{\frac{\lambda^5}{\pi}} \, r \cos\theta \, e^{-\lambda r} \,. \tag{66}$$

Here λ is the Slater orbital index, taken to be 2.18 in calculations. Substituting Eq.(66) into Eqs. (10), (14), (15), (17), (18) and (19) and noting that the bond lengths between carbon atoms are different from the undeformed graphene, we can obtain the analytical expressions for the hopping and overlap integrals (Wei & Tong, 2009). Because the bond lengths are dependent of force f, the hopping and overlap integrals depend on the force. Fig.10 shows the change of the energy gap with tensile force f_N at Dirac points K, where the third neighbor is included. The Dirac points will vary with the force, for zigzag ribbons given by

$$K = \left(\frac{\pi}{d_2 \cos\alpha + d_1}, \frac{\pi}{2d_2 \sin\alpha} - \frac{\pi d_2 \sin\alpha}{2(d_2 \cos\alpha + d_1)^2} \right),$$

$$K' = \left(\frac{\pi}{d_2 \cos\alpha + d_1}, \frac{\pi d_2 \sin\alpha}{2(d_2 \cos\alpha + d_1)^2} - \frac{\pi}{2d_2 \sin\alpha} \right). \qquad (67)$$

It is clear that a pulling force may make Dirac points opening an energy gap, and which varies nonlinearly as the force. When the force is small, the change of the gap nearly is linear. But as the force becomes large, this change appears nonlinear. By comparison, we see that the gap of zigzag edges is more than that of armchair edges under the same force. This means that the gap of wider graphene ribbons with zigzag shaped edges is easily opened by an external force with respect to the armchair edges.

6. Conclusion

In this chapter, we study in details the electronic energy dispersion relations of graphene and its nanoribbons within the tight binding model, including up to the third-neighbor interaction. For a graphene sheet, there are no energy gaps at high-symmetry points K. The next-nearest-neighbor hopping integrals and wave function overlap between carbon atoms impact strongly on the bandwidth, i.e., their effects make the bandwidth become narrow with respect to the nearest neighbor result. The third neighbors can increase the bandwidth slightly and decrease the energy difference between the lowest conduction and highest valence bands greatly. The electronic dispersion of armchair edge graphene nanoribbons is given analytically based on the tight binding approach and hard-wall boundary condition. For the armchair nanoribbon, different widths have different dispersion relations. When $n=3m$ and $n=3m+1$, the second neighbor terms are able to reduce the bandwidth and slightly increase the band gap at Γ point. In general, smaller quantum number q impacts on the bandwidth and larger q affects the band gap. The effect of the third neighbor interaction is opposite to that of the second neighbor, but a flat band disappears when we involve the third neighbors. As for $n=3m+2$, the non-neighbor interaction can not open the gap at Dirac point. We also evaluate the influence of the edge deformation on this ribbon and compare the competition between both the non-neighbor interaction and edge deformation in energy gaps. For zigzag nanoribbons, there is no energy gap and the non-neighbor interaction impacts only on the bandwidth. In addition, the energy gaps of graphene ribbons with armchair or zigzag edges can be opened by an external force. Opening the gap of the zigzag edge ribbon is easier with respect to the armchair ribbon.

The problem we discussed above is the ideal graphene nanoribbons. If we consider the warping of the edges and the non-flat ribbon, the energy dispersion would how to change? These issues are worthy of further study.

7. References

Brey, L. & Fertig, H. A. (2006). Electronic states of graphene nanoribbons studied with the Dirac equation. *Phys. Rev.* B73, 23, 235411(1-5), 1550-235x

Castro Neto, A. H.; Guinea, F.; Peres, N. M. R.; Novoselov, K. S. & Geim, A. K. (2009). The electronic properties of graphene. *Reviews of Modern Physics,* 81, 1, 109-162, 1539-0756

Fujita, M.; Wakabayashi, K.; Nakada, K. & Kusakabe, K. (1996). Peculiar localized state at zigzag graphite edge. *J. Phys. Soc. Jpn.*, 65, 7, 1920-1923

Geim, A. K. & Novoselov, K. S. (2007). The rise of graphene. *Nature Materials* , 6, 183-191, 1476-4660

Jin, Z. F.; Tong, G. P. & Jiang, Y. J. (2009). Effect of the non-nearest-neighbor hopping on the electronic structure of armchair graphene nanoribbons. *Acta Physica Sinica*, 58, 12, 8537-8543, 1000-3290

Lomer, W. M. (1955). The Valence Bands in Two-Dimensional Graphite. *Proc. Roy. Soc. (London)*, A227, 1170, 330-349, 1471-2946

McClure, J. W. (1956). Diamagnetism of graphite. *Phys. Rev.* 104, 3, 666-671,

Nakada, K.; Fujita, M.; Dresselhaus, G. & Dresselhaus, M. S. (1996). Edge state in graphene ribbons: Nanometer size effect and edge shape dependence. *Phys. Rev*. B54, 24, 17954-17961, 1550-235x

Novoselov, K. S.; Geim, A. K.; Morozov, S. V.; Jiang, D.; Zhang, Y.; Dubonos, S. V.; Grigorieva, I. V. & Firsov , A. A. (2004) . *Science*, 306, 5696, 666-669, 1095-9203

Novoselov, K. S.; Geim, A. K.; Morozov, S. V.; Jiang, D.; Katsnelson, M. I.; Grigorieva, I. V.; Dubonos, S. V. & Firsov, A. A. (2005). Two-dimensional gas of massless Dirac fermions in graphene. *Nature*, 438, 197-200, 0028-0836

Porezag, D.; Frauenheim, T.; Kohler, T.; Seifert, G. & Kaschner, R. (1995). Construction of tight-binding-like potentials on the basis of density-functional theory: Application to carbon. *Phys. Rev*. B51, 19, 12947-12957, 1550-235x

Reich, S; Maultzsch, J. & Thomsen, C. (2002). Tight-binding description of graphene. *Phys. Rev*. B66, 3, 035412(5), 1550-235x

Rozhkov, A. V.; Savel'ev, S. & Nori, F. (2009). Electronic properties of armchair graphene nanoribbons. *Phys. Rev.*, B79, 12, 125420(10), 1550-235x

Saito, R.; Dresselhaus, D. & Dresselhaus, M. S. (1998). *Physical Properties of Carbon Nanotubes*, Imperial College Press, 1-86094-093-5, London

Slonczewski, J.C. & Weiss, P.R. (1958). Band structure of graphite. *Phys. Rev.* 109, 2, 272-279,

Son, Y. W.; Cohen, M. L. & Louie, S. G. (2006). Energy gaps in graphene nanoribbons. *Phys. Rev. Lett*., 97, 21, 216803(1-4), 1079-7114

Wallace, P. R. (1947). The band theory of graphite. *Phys. Rev.* 71, 9, 622-634

Wei, Y. & Tong, G. P. (2009). Effect of the tensile force on the electronic energy gap of graphene sheets. *Acta Physica Sinica*, 58, 3, 1931-1934, 1000-3290

Zheng, H. X.; Wang, Z. F.; Luo, T.; Shi, Q. W. & Chen, J. (2007). Analytical study of electronic structure in armchair graphene nanoribbons. *Phys. Rev.* B75, 16, 165411(1-6), 1550-235x
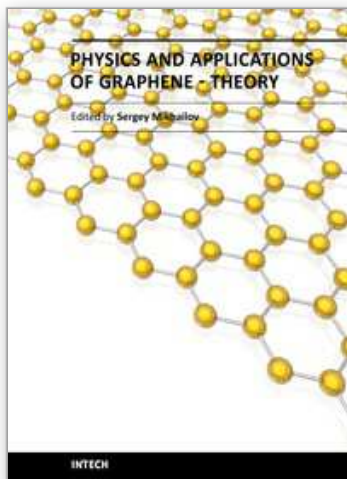
Physics and Applications of Graphene - Theory

Edited by Dr. Sergey Mikhailov

The Stone Age, the Bronze Age, the Iron Age... Every global epoch in the history of the mankind is characterized by materials used in it. In 2004 a new era in material science was opened: the era of graphene or, more generally, of two-dimensional materials. Graphene is the strongest and the most stretchable known material, it has the record thermal conductivity and the very high mobility of charge carriers. It demonstrates many interesting fundamental physical effects and promises a lot of applications, among which are conductive ink, terahertz transistors, ultrafast photodetectors and bendable touch screens. In 2010 Andre Geim and Konstantin Novoselov were awarded the Nobel Prize in Physics "for groundbreaking experiments regarding the two-dimensional material graphene". The two volumes Physics and Applications of Graphene - Experiments and Physics and Applications of Graphene - Theory contain a collection of research articles reporting on different aspects of experimental and theoretical studies of this new material.

How to reference

In order to correctly reference this scholarly work, feel free to copy and paste the following:

Tong Guo-Ping (2011). The Non-Neighbor Effect in Graphene Ribbons, Physics and Applications of Graphene - Theory, Dr. Sergey Mikhailov (Ed.), ISBN: 978-953-307-152-7, InTech, Available from: http://www.intechopen.com/books/physics-and-applications-of-graphene-theory/the-non-neighbor-effect-in-graphene-ribbons

INTECH
open science | open minds